# A Low Complexity PAPR Reduction Method Based on FWFT and PEC for OFDM Systems

Ce Kang, Yi Liu, Meixia Hu, and Hailin Zhang

***Abstract*—Orthogonal frequency division multiplexing (OFDM) is a multi-carrier modulation technique for transmitting large volumes of digital data but suffers high peak-to-average power ratio (PAPR) at the transmitter. In this paper, we propose a PAPR reduction technique based on the combination of a low complexity transform-Fast Walsh–Hadamard and Fourier transform (FWFT) and the parameter-adjustable piecewise exponential companding (PEC). To reduce algorithm complexity, FWFT uses a fast orthonormal unitary transform to calculate both the Walsh–Hadamard transform (WHT) and the discrete Fourier transform (DFT). In FWFT, WHT realizes precoding to OFDM signals and as a result the PAPR is reduced first. Moreover, the parameter-adjustable PEC transform is adopted to further reduce PAPR by transforming the statistics of the companded signal into exponential distribution with adjustable parameters. Simulation results show that the hybrid method achieves significant PAPR reduction and improves the BER performance of OFDM systems when used in multipath fading channels.**

***Index Terms*—Transform-fast Walsh–Hadamard and Fourier transform (FWFT), piecewise exponential companding (PEC), orthogonal frequency division multiplexing (OFDM), peak-to-average power ratio (PAPR), Walsh–Hadamard.**

## I. Introduction

ORTHOGONAL frequency division multiplexing (OFDM) is extensively adopted in practical wireless communication systems for its advantages of robustness against narrow band interference and frequency selective fading, high spectral efficiency, high quality service and good design flexibility. Nowadays, OFDM has developed into a popular technique for wideband digital communications, adopted in applications such as digital television and audio broadcasting, digital subscriber line (DSL) Internet access, wireless local area networks (WLAN), 4G wireless communication systems and wireline digital communication systems.

However, the high peak-to-average power ratio (PAPR) is still one of the major drawbacks of OFDM, which may cause high power amplifiers (HPA) to operate in nonlinear region and to produce nonlinear distortion, such as spectral regrowth and intersymbol interference. To solve the problem of PAPR, various techniques have been proposed, such as clipping and filtering [1]–[3], companding [4], [5], selective mapping [6], [7], partial transmit sequence [8], [9], and precoding based techniques [10], [11]. Among these techniques, companding techniques have gained great attentions owing to their low complexity and high bandwidth efficiency. Various companding schemes with uniform transform have been proposed [12]–[14]. Jiang *et al.* [12] proposed the well-known exponential companding (EC) scheme. By transforming the Rayleigh distributed OFDM signal into a uniform distributed signal, EC scheme can reduce PAPR greatly. Moreover, EC scheme can offer design freedom in the PAPR reduction with an adjustable parameter which determines the distribution of the companded signals. However, when EC scheme is adopted, unnecessary compression is operated on small signals, which causes the deterioration of BER and PSD performance. To overcome this defect, some researchers proposed companding schemes with piecewise transform [15], [16]. The piecewise companding (PC) scheme proposed in [15] focuses on transforming the distribution of large signals to reduce the degeneration of BER and PSD performance. Wang *et al.* [16] proposed a piecewise non-linear companding scheme with more design freedom and flexibility to achieve a better tradeoff between the PAPR reduction and the BER and PSD performance.

Companding is a non-linear process and may cause serious in-band distortion which may cause great BER degradation. Regarding BER performance improvement, some researchers have proposed hybrid methods which combine precoding and companding [17]–[20]. Adding WHT to an OFDM system can reduce the influence of the selective fading channel on system performance, which has been demonstrated in [21] and [22]. Xiao *et al.* [17] proposed a hybrid method, which combines WHT precoding and $\mu$-law companding to reduce PAPR of OFDM systems while maintaining BER performance. Elmaroud *et al.* [18] proposed the combination of WHT precoding and exponential companding to achieve PAPR reduction of FBMC signals. However, the complexity of these hybrid methods was high owing to the utilization of IFFT and the WHT separately.

In this paper, we propose a PAPR reduction technique based on the combination of the parameter-adjustable piecewise exponential companding (PEC) with a low complexity transform-FWFT. The PEC scheme deals with the small and large signals differently. It only transforms the distribution of the large signals into exponential distribution and there

Manuscript received June 23, 2016; revised November 26, 2016; accepted December 2, 2016. Date of publication January 11, 2017; date of current version June 3, 2017. This work was supported in part by the Natural Science Foundation of China under Grant 61671341, Grant 61301169, and Grant 61401330, in part by the China Post-Doctoral Science Foundation under Grant 2014M562373, and in part by the 111 Project of China under Grant B08038.

The authors are with the State Key Laboratory of Integrated Service Network, Xidian University, Xi'an 710071, China (e-mail: stephenkang@foxmail.com; yliu@xidian.edu.cn; hlzhang@xidian.edu.cn; mxhu@mail.xidian.edu.cn).

Digital Object Identifier 10.1109/TBC.2016.2637278

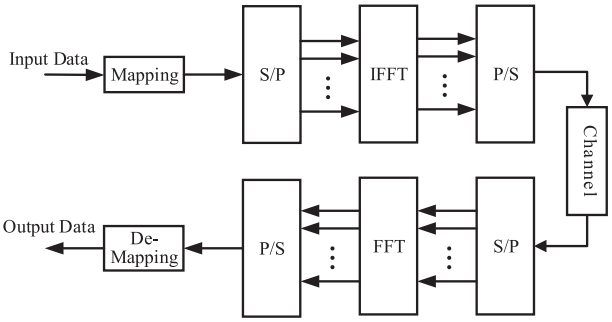


Fig. 1. Block diagram of a baseband OFDM system.

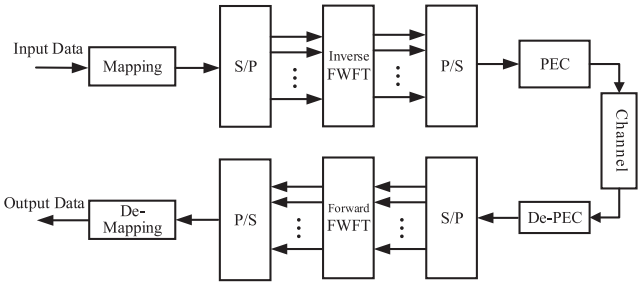


Fig. 2. Block diagram of the proposed OFDM system with PAPR reduction.

| $M$ | | | | $N$ |
|---|---|---|---|---|
| 0 | $(0000)_2$ | $\rightarrow$ | $(0000)_2$ | 0 |
| 1 | $(0001)_2$ | $\rightarrow$ | $(1000)_2$ | 8 |
| 2 | $(0010)_2$ | $\rightarrow$ | $(0100)_2$ | 4 |
| | | $\vdots$ | | |
| 14 | $(1110)_2$ | $\rightarrow$ | $(0111)_2$ | 7 |
| 15 | $(1111)_2$ | $\rightarrow$ | $(1111)_2$ | 15 |

Fig. 3. Bit reverse order for $N = 16$. ($M$ denotes row/column number in original order and $N$ denotes row/column number in bit reverse order).

is no companding operation on small signals. Therefore, the PEC scheme can greatly suppress PAPR while reducing the signal distortion. Moreover, utilizing an inflexion point and transform parameters, the PEC scheme offers more design freedom. FWFT can calculate DFT and WHT together efficiently. Different from simple cascade of WHT and IFFT in other techniques, FWFT employs a fast algorithm to calculate both Walsh-Hadamard and Fourier transform. Another advantage of using FWFT in OFDM systems is PAPR is further reduced to some extent because FWFT introduces some correlation between subcarriers. Moreover, FWFT which contains WHT can improve BER performance of the hybrid system in multipath fading channels. Combining the advantages of PEC and FWFT, the hybrid scheme can achieve significant PAPR reduction and reasonable BER improvement with low computational complexity.

The paper is organized as follows: Section II describes the system model. The PAPR reduction scheme is presented in Section III. In Section IV, simulation results are provided and discussed. Section V concludes the paper.

## II. PAPR of OFDM Systems

A baseband OFDM system is shown in Fig. 1, where each OFDM symbol consists of $N$ subcarriers. The modulated symbols pass through Serial/Parallel converter which generates complex vector of size $N$. The vector can be written as $\mathbf{X} = [X_0, X_1, \ldots, X_{N-1}]^T$ and then $\mathbf{X}$ passes through the IFFT block. The complex baseband OFDM signal can be written as

$$x_n = \frac{1}{\sqrt{N}} \sum_{k=0}^{N-1} X_k e^{\frac{j2\pi kn}{N}}, 0 \le n < N. \tag{1}$$

In time domain, the signal $x_n$ is actually the mixed signal of $N$ independent subcarriers. Thus the OFDM signal $x_n$ occasionally exhibits very high peaks which can be measured by PAPR. The PAPR is defined as the ratio of maximum signal power to average signal power.

$$PAPR = 10 \log \frac{\max\{|x_n|\}^2}{avg\{|x_n|\}^2}. \tag{2}$$

In general, the performance of PAPR reduction is measured by the complimentary cumulative distribution function (CCDF) which is defined as the probability that the PAPR of signal exceeds an assigned threshold. Assuming $PAPR_0$ is the threshold value, CCDF can be expressed as follows,

$$CCDF = Pr(PAPR > PAPR_0). \tag{3}$$

## III. Proposed PAPR Reduction Method

The proposed OFDM system with hybrid PAPR reduction is shown in Fig. 2. We denote the modulated signal vector as $\mathbf{X} = [X_0, X_1, \ldots, X_{N-1}]^T$. Processed by inverse FWF-transform, $\mathbf{X}$ can be written as

$$\mathbf{x} = \mathbf{T}'\mathbf{X}, \tag{4}$$

where $\mathbf{T}' = \frac{1}{N}\mathbf{F}'\mathbf{W}$ is the $N \times N$ FWF-transform matrix, $\mathbf{F}$ and $\mathbf{W}$ being the $N$ point IDFT matrix rearranged by row bit reverse order as shown in Fig. 3 and the WHT matrix, respectively. After CP added, the output of the signal $\mathbf{x} = [x_0, x_1, \ldots, x_{N-1}]^T$ passing through parameter-adjustable piecewise exponential companding can be written as

$$\mathbf{s} = C(\mathbf{x}), \tag{5}$$

where $C(\cdot)$ denotes the PEC function and $\mathbf{s}$ is the signal to be sent into wireless channels. Assuming $\mathbf{h}$ is the channel impulse response and $\mathbf{n}$ is the additive white Gaussian noise, the received signal after removing CP can be expressed as

$$\mathbf{r} = \mathbf{s} * \mathbf{h} + \mathbf{n}. \tag{6}$$

With the de-companding operation, the recovered signal can be expressed as

$$\mathbf{y} = C^{-1}(\mathbf{r}). \tag{7}$$

Then $\mathbf{y}$ is fed into the forward FWF-transform block and the signal after this transform is

$$\mathbf{Y} = \mathbf{T}\mathbf{y}, \tag{8}$$

where $\mathbf{T} = \frac{1}{N}\mathbf{W}\mathbf{F}$ is the forward FWF-transform matrix, $\mathbf{F}$ and $\mathbf{W}$ being the $N$ point DFT matrix rearranged by column bit reverse order and the WHT matrix, respectively. Then the signal $\mathbf{Y}$ is demodulated to a bit stream.

The proposed scheme includes two stages of PAPR reduction. One is FWFT and the other is the parameter-adjustable

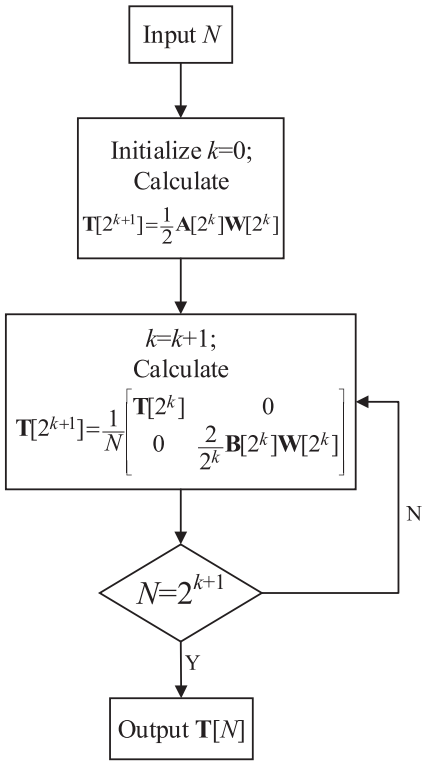


Fig. 4. Flow diagram of the algorithm for generating $\mathbf{T}[N]$.

piecewise exponential companding in (5). Next, the scheme will be described in detail.

### A. Fast Walsh-Hadamard and Fourier Transform (FWFT)

FWFT and IFWFT are adopted instead of FFT and IFFT. In FWFT or IFWFT, we use a fast algorithm to calculate Walsh-Hadamard and Fourier transforms simultaneously. Let us take IFWFT used in transmitting end as an example. From [24], the IFWFT matrix $\mathbf{T}$ of size $N$ can be expressed as

$$\mathbf{T}[N]=\frac{1}{N}\begin{bmatrix}\mathbf{T}\left[\frac{N}{2}\right] & 0\\ 0 & \left(\frac{2}{N}\right)\mathbf{B}\left[\frac{N}{2}\right]\mathbf{W}\left[\frac{N}{2}\right]\end{bmatrix}. \tag{9}$$

By iterating on the upper half, it is not hard to see $\mathbf{T}[N]$ can be expressed as (10) at the top of the next page. As Fig. 4 shows, we can obtain $\mathbf{T}[N]$ by following the flow diagram of the algorithm.

Assume $\mathbf{F}[2^{k+1}]$ and $\mathbf{W}[2^{k+1}]$ are the IDFT matrices rearranged by row reverse order and the Walsh-Hadamard matrix in size $N=2^{k+1}$, respectively. $\mathbf{A}[2^k]$, $\mathbf{B}[2^k]$, and $\mathbf{W}[2^k]$ denote the submatrices of $\mathbf{F}[2^{k+1}]$ and $\mathbf{W}[2^{k+1}]$ as follows,

$$\mathbf{F}\left[2^{k+1}\right]=\frac{1}{2^{k+1}}\begin{bmatrix}\mathbf{A}\left[2^k\right] & \mathbf{A}\left[2^k\right]\\ \mathbf{B}\left[2^k\right] & -\mathbf{B}\left[2^k\right]\end{bmatrix}, \tag{11}$$

$$\mathbf{W}\left[2^{k+1}\right]=\begin{bmatrix}\mathbf{W}\left[2^k\right] & \mathbf{W}\left[2^k\right]\\ \mathbf{W}\left[2^k\right] & -\mathbf{W}\left[2^k\right]\end{bmatrix}. \tag{12}$$

From (10), we can see $\mathbf{T}[N]$ is a block diagonal matrix with two thirds of its elements being zero. The number of multiplications and additions involved in the calculation of the IFWFT matrices is already far less than that of those involved in the IDFT matrices.

In implementation, we can further factorize $\mathbf{T}$ into sparse matrices and use a new butterfly algorithm to achieve a faster transform calculation. Consider for instance the case of $N=16$ and $\mathbf{T}[16]$ can be written as follows,

$$\mathbf{T}[16]=\frac{1}{16}\begin{bmatrix}\frac{1}{2}\mathbf{A}[2]\mathbf{W}[2] & 0 & 0 & 0\\ 0 & \frac{1}{2}\mathbf{B}[2]\mathbf{W}[2] & 0 & 0\\ 0 & 0 & \frac{1}{4}\mathbf{B}[4]\mathbf{W}[4] & 0\\ 0 & 0 & 0 & \frac{1}{8}\mathbf{B}[8]\mathbf{W}[8]\end{bmatrix}. \tag{13}$$

In $\mathbf{T}[16]$, the submatrix $\frac{1}{8}\mathbf{B}[8]\mathbf{W}[8]$ can be expressed as follows,

$$\begin{aligned}&\frac{1}{8}\mathbf{B}[8]\mathbf{W}[8]\\ &\quad=\begin{bmatrix}\frac{1}{8}\left(1+w^4\right)\mathbf{D}[4]\mathbf{W}[4] & \frac{1}{8}\left(1-w^4\right)\mathbf{E}[4]\mathbf{W}[4]\\ \frac{1}{8}\left(1-w^4\right)\mathbf{D}[4]\mathbf{W}[4] & \frac{1}{8}\left(1+w^4\right)\mathbf{E}[4]\mathbf{W}[4]\end{bmatrix},\end{aligned} \tag{14}$$

where **D[4]** and **E[4]** can be respectively written as

$$\mathbf{D}[4]=\begin{bmatrix}1 & w^1 & w^2 & w^3\\ 1 & -w^1 & w^2 & -w^3\\ 1 & w^5 & -w^2 & -w^7\\ 1 & -w^5 & -w^2 & w^7\end{bmatrix}, \tag{15}$$

$$\mathbf{E}[4]=\begin{bmatrix}1 & w^3 & w^6 & -w^1\\ 1 & -w^3 & w^6 & w^1\\ 1 & w^7 & -w^6 & w^5\\ 1 & -w^7 & -w^6 & -w^5\end{bmatrix}. \tag{16}$$

Define $w=e^{\frac{j2\pi}{N}}$, $P1=\frac{1+w^4}{2}$, $P2=\frac{1-w^4}{2}$, $P3=\frac{1+w^2}{2}$, $P4=\frac{1-w^2}{2}$, $P5=\frac{1+w^6}{2}$, $P6=\frac{1-w^6}{2}$, $P7=\frac{1+w}{2}$, $P8=\frac{1-w}{2}$, $P9=\frac{1+w^5}{2}$, $P10=\frac{1-w^5}{2}$, $P11=\frac{1+w^3}{2}$, $P12=\frac{1-w^3}{2}$, $P13=\frac{1+w^7}{2}$, and $P14=\frac{1-w^7}{2}$.

Then, $\frac{1}{2}\mathbf{A}[2]\mathbf{W}[2]$ and $\frac{1}{2}\mathbf{B}[2]\mathbf{W}[2]$ can be respectively obtained as

$$\frac{1}{2}\mathbf{A}[2]\mathbf{B}[2]=\begin{bmatrix}1 & 0\\ 0 & 1\end{bmatrix}, \tag{17}$$

$$\frac{1}{2}\mathbf{B}[2]\mathbf{W}[2]=\frac{1}{2}\begin{bmatrix}P2 & P1\\ P1 & P2\end{bmatrix}. \tag{18}$$

Also, $\frac{1}{4}\mathbf{B}[4]\mathbf{W}[4]$ can be written as

$$\begin{aligned}&\frac{1}{4}\mathbf{B}[4]\mathbf{W}[4]\\ &=\frac{1}{4}\begin{bmatrix}1 & w^2 & w^4 & w^6\\ 1 & -w^2 & w^4 & -w^6\\ 1 & w^6 & -w^4 & w^2\\ 1 & -w^6 & -w^4 & -w^2\end{bmatrix}\times\begin{bmatrix}1 & 1 & 1 & 1\\ 1 & -1 & 1 & -1\\ 1 & 1 & -1 & -1\\ 1 & -1 & -1 & 1\end{bmatrix}\\ &=\begin{bmatrix}P3 & P4 & 0 & 0\\ P4 & P3 & 0 & 0\\ 0 & 0 & P5 & P6\\ 0 & 0 & P6 & P5\end{bmatrix}\times\begin{bmatrix}P1 & 0 & P2 & 0\\ 0 & P1 & 0 & P2\\ P2 & 0 & P1 & 0\\ 0 & P2 & 0 & P1\end{bmatrix}.\end{aligned} \tag{19}$$

$$\mathbf{T}[N]=\frac{1}{N}\begin{bmatrix}\frac{1}{2}\mathbf{A}[2]\mathbf{W}[2] & 0 & 0 & \cdots & 0 & 0\\ 0 & \frac{1}{2}\mathbf{B}[2]\mathbf{W}[2] & 0 & \cdots & 0 & 0\\ 0 & 0 & \frac{1}{4}\mathbf{B}[4]\mathbf{W}[4] & \cdots & 0 & 0\\ \ddots & \ddots & \ddots & \cdots & \ddots & \ddots\\ 0 & 0 & 0 & \cdots & \frac{4}{N}\mathbf{B}\left[\frac{N}{4}\right]\mathbf{W}\left[\frac{N}{4}\right] & 0\\ 0 & 0 & 0 & \cdots & 0 & \frac{2}{N}\mathbf{B}\left[\frac{N}{2}\right]\mathbf{W}\left[\frac{N}{2}\right]\end{bmatrix} \tag{10}$$

In the same way, $\frac{1}{8}(1+w^4)\mathbf{D}[4]\mathbf{W}[4]$ in (14) can be written as (20) at the bottom of the next page.

We can see the first two matrices of the right hand side in (20) share the same structure with the two matrices in (19), with elements of the matrix P3 replaced by P7, P4 replaced by P8, P5 replaced by P9, P6 replaced by P10, P1 replaced by P3, and P2 replaced by P4.

Similarly, the other three submatrices in (14) can be evaluated as

$$\begin{aligned}&\frac{1}{8}\left(1-w^4\right)\mathbf{E}[4]\mathbf{W}[4]\\ &=\begin{bmatrix}P11 & P12 & 0 & 0\\ P12 & P11 & 0 & 0\\ 0 & 0 & P13 & P14\\ 0 & 0 & P14 & P13\end{bmatrix}\times\begin{bmatrix}P5 & 0 & P6 & 0\\ 0 & P5 & 0 & P6\\ P6 & 0 & P5 & 0\\ 0 & P6 & 0 & P5\end{bmatrix}\\ &\quad\times\begin{bmatrix}P2 & 0 & 0 & 0\\ 0 & P2 & 0 & 0\\ 0 & 0 & P2 & 0\\ 0 & 0 & 0 & P2\end{bmatrix},\end{aligned} \tag{21}$$

$$\begin{aligned}&\frac{1}{8}\left(1-w^4\right)\mathbf{D}[4]\mathbf{W}[4]\\ &=\begin{bmatrix}P7 & P8 & 0 & 0\\ P8 & P7 & 0 & 0\\ 0 & 0 & P9 & P10\\ 0 & 0 & P10 & P9\end{bmatrix}\times\begin{bmatrix}P3 & 0 & P4 & 0\\ 0 & P3 & 0 & P4\\ P4 & 0 & P3 & 0\\ 0 & P4 & 0 & P3\end{bmatrix}\\ &\quad\times\begin{bmatrix}P2 & 0 & 0 & 0\\ 0 & P2 & 0 & 0\\ 0 & 0 & P2 & 0\\ 0 & 0 & 0 & P2\end{bmatrix},\end{aligned} \tag{22}$$

$$\begin{aligned}&\frac{1}{8}\left(1+w^4\right)\mathbf{E}[4]\mathbf{W}[4]\\ &=\begin{bmatrix}P11 & P12 & 0 & 0\\ P12 & P11 & 0 & 0\\ 0 & 0 & P13 & P14\\ 0 & 0 & P14 & P13\end{bmatrix}\times\begin{bmatrix}P5 & 0 & P6 & 0\\ 0 & P5 & 0 & P6\\ P6 & 0 & P5 & 0\\ 0 & P6 & 0 & P5\end{bmatrix}\\ &\quad\times\begin{bmatrix}P1 & 0 & 0 & 0\\ 0 & P1 & 0 & 0\\ 0 & 0 & P1 & 0\\ 0 & 0 & 0 & P1\end{bmatrix}.\end{aligned} \tag{23}$$

By this means, we can further factorize $\mathbf{T}$ into sparse matrices and this method can be extended to any transform length. Denoting $\omega_n=\frac{1-e^{j2\pi\frac{n}{N}}}{2}$, a flowchart of the 16 point ($N=16$) FWF-transform is shown in Fig. 5. The structure of each butterfly is shown in Fig. 6, where $o_1$ and $o_2$ denote the output data of each butterfly and can be calculated as $o_1=i_1-(i_1-i_2)\omega_n$ and $o_2=i_2+(i_1-i_2)\omega_n$, respectively.

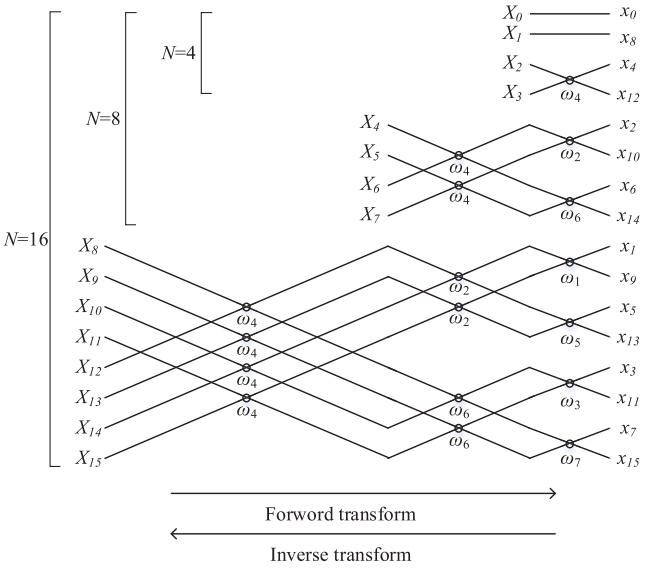


Fig. 5. FWF-transform flowchart for the example of $N=16$.

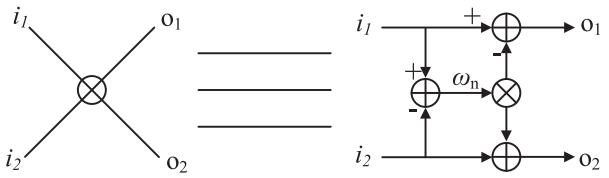


Fig. 6. Structure diagram of a single butterfly.

*1) Computational Complexity:* From Fig. 5, it can be deduced that $\frac{1}{2}[N\log_2(N)-(2N-2)]$ butterflies are required for an $N$ point FWF-transform. It is not hard to see one complex multiplication and three complex additions are involved in the calculation of each butterfly. Therefore, the total number of complex multiplications $C_{Mults}$ and additions $C_{Adds}$ can be calculated as follows,

$$C_{Mults}=\frac{1}{2}\left[N\log_2(N)-(2N-2)\right], \tag{24}$$

$$C_{Adds}=\frac{3}{2}\left[N\log_2(N)-(2N-2)\right]. \tag{25}$$

TABLE I
REAL ARITHMETIC OPERATIONS OF A SINGLE BUTTERFLY IMPLEMENTATIONIN IN OFDM, WHT-OFDM, AND FWF-OFDM

| | Real multiplication | Real addition |
|---|---|---|
| OFDM | $2N\log_2 N$ | $3N\log_2 N$ |
| FWF-OFDM | $2[N\log_2 N-(2N-2)]$ | $4[N\log_2 N-(2N-2)]$ |
| WHT-OFDM | $2N\log_2 N$ | $5N\log_2 N$ |

One complex multiplication can be implemented using either four real multiplications and two real additions or three real multiplications and three real additions. In this paper, we consider the complexity of one complex multiplication is equivalent to the complexity of four real multiplications and two real additions. Moreover, one complex addition is equivalent to two real additions. Therefore, the total number of real multiplications $R_{Mults}$ and additions $R_{Adds}$ can be calculated as follows,

$$R_{Mults} = 2\big[N\log_2(N) - (2N-2)\big], \tag{26}$$

$$R_{Adds} = 4\big[N\log_2(N) - (2N-2)\big]. \tag{27}$$

The comparison about real arithmetic operations among transforms in OFDM, WHT-OFDM, and FWF-OFDM is shown in Table I.

*2) PAPR Reduction Analysis:* According to (2), the PAPR of time domain OFDM signal samples can be written as

$$PAPR[x(n)] = 10\log\frac{\max\limits_{0\le n\le N-1}\big[|x_n|^2\big]}{E\big[|x_n|^2\big]}, \tag{28}$$

where $N$ denotes the number of the subcarrier. From (28), we can see the PAPR of OFDM signal is determined by the average power and peak power. The average power $E[|\mathbf{x^2}|]$ can be calculated as

$$E\Big[\Big|\mathbf{x}^2\Big|\Big] = E\big(\mathbf{x}\mathbf{x}^*\big) = E\big[\big(\mathbf{T}'\mathbf{X}\big)\big(\mathbf{T}\mathbf{X}'\big)\big]. \tag{29}$$

Substituting $\mathbf{T} = \frac{1}{N}\mathbf{F}'\mathbf{W}$ into (29), $E[|\mathbf{x}|^2]$ can be written as

$$\begin{aligned} E\Big[|\mathbf{x}|^2\Big] &= E\Bigg[\bigg(\frac{1}{N}\sum_{k=0}^{N-1}\sum_{m=0}^{N-1}X_m W_{m,k}F_{k,n}\bigg) \\ &\qquad \bigg(\frac{1}{N}\sum_{k=0}^{N-1}\sum_{m=0}^{N-1}X_m^* W_{m,k}^* F_{k,n}^*\bigg)\Bigg] \\ &= \frac{1}{N}\sum_{m=0}^{N-1}|X_m|^2. \end{aligned} \tag{30}$$

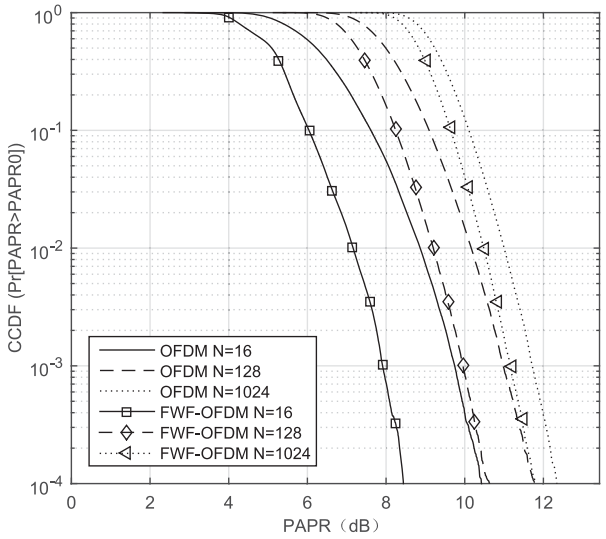


Fig. 7. CCDF of OFDM and FWF-OFDM systems with different numbers of subcarriers.

From (30), we can see the average power is constant after signals passing through FWFT, the same as after passing through IFFT. So the peak power reduction determines the level of PAPR reduction. In traditional OFDM systems, when processed through IFFT, the peak power of the output signals can be high because of the superposition of the input signals. For an $N$ subcarriers OFDM system, there are $\log_2(N)$ stages involved in IFFT. In FWF-OFDM systems, as Fig. 5 shows, FWFT involves $\log_2(N)-1$ stages only, which are less than in IFFT. Moreover, FWFT has a block diagonal structure with $\log_2(N)-1$ sections and two direct paths. And more than half of elements in each section are zero. As a result, the superposition of the input signals in FWFT is less than that in IFFT, which leads to a lower peak power. Therefore, FWFT achieves better PAPR performance compared with IFFT.

In OFDM systems, according to the central limit theorem, we can approximate the distribution of each peak of the signal after IFFT as Gaussian distribution when $N$ is large enough. As for FWF-OFDM systems, when the number of subcarriers increases, the number of sections in FWFT matrices with Gaussian distributions increases, so the overall distribution of the output signal after passing through FWFT can also be approximated as Gaussian. Thus, for a larger $N$, the peak of the FWF-OFDM system is closer to that of the OFDM system. In conclusion, as the number of subcarriers $N$

$$\begin{aligned} \frac{1}{8}\Big(1+w^4\Big)\mathbf{D}[4]\mathbf{W}[4] &= \frac{1}{8}(1+w^4)\begin{bmatrix}1 & w^1 & w^2 & w^3\\ 1 & -w^1 & w^2 & -w^3\\ 1 & w^5 & -w^2 & -w^7\\ 1 & -w^5 & -w^2 & w^7\end{bmatrix}\times\begin{bmatrix}1 & 1 & 1 & 1\\ 1 & -1 & 1 & -1\\ 1 & 1 & -1 & -1\\ 1 & -1 & -1 & 1\end{bmatrix} \\ &= \begin{bmatrix}P7 & P8 & 0 & 0\\ P8 & P7 & 0 & 0\\ 0 & 0 & P9 & P10\\ 0 & 0 & P10 & P9\end{bmatrix}\times\begin{bmatrix}P3 & 0 & P4 & 0\\ 0 & P3 & 0 & P4\\ P4 & 0 & P3 & 0\\ 0 & P4 & 0 & P3\end{bmatrix}\times\begin{bmatrix}P1 & 0 & 0 & 0\\ 0 & P1 & 0 & 0\\ 0 & 0 & P1 & 0\\ 0 & 0 & 0 & P1\end{bmatrix} \end{aligned} \tag{20}$$

$$h(x) = \begin{cases} x, & |x| < A_i \\ \operatorname{sgn}(x)\left(\left(A_i^d - A_c^d\right)e^{-\left(|x_n|^2 - A_i^2\right)/\sigma^2} + A_c^d\right)^{(1/d)}, & |x| \geq A_i \end{cases} \tag{31}$$

increases, the PAPR performance of FWF-OFDM is closer to that of traditional OFDM as shown in Fig. 7.

### *B. Parameter-Adjustable Piecewise Exponential Companding*

Although FWFT, which functions as WHT precoding, can reduce PAPR to a certain extent, PAPR may be still high because WHT precoding does not take the signal property into consideration. To further reduce PAPR, a parameter-adjustable piecewise exponential companding is adopted to this system. In this section, we review the parameter-adjustable piecewise exponential companding (PEC) technique which was first proposed by us in [23], and which has been proved to achieve significant PAPR reduction.

The PEC scheme deals with the small and large signals differently. It only transforms the distribution of the large signals into exponential distribution and there is no companding operation on small signals. Moreover, by utilizing an inflexion point and transform parameters, the PEC scheme can offer more design flexibility, and therefore achieves a better tradeoff among the PAPR reduction, BER, and PSD performance. We denote the inflexion point of PEC as $A_i$. Assume $\sigma^2$ denotes the power of the input signal $x_n$, $A_c$ is the cutoff point, and $d$ is the degree of the companding scheme. The PEC function at the transmitter can be expressed as (31) at the top of this page.

At the receiver, the de-companding function can be expressed as

$$h^{-1}(x) = \begin{cases} x, & |x| < A_i \\ \operatorname{sgn}(x)\sqrt{A_i^2 - \sigma^2 \ln\left(\frac{|x|^d - A_c^d}{A_i^d - A_c^d}\right)}, & |x| \geq A_i, \end{cases} \tag{32}$$

where $\operatorname{sgn}(\cdot)$ denotes the sign function.

Among these parameters in PEC, $A_c$ can be determined by the preset PAPR value as $A_c = \sigma \times 10^{(PAPR_{preset}/20)}$ . With the determined $A_c$ , once $d$ is selected, the parameters $A_i$ can be obtained by solving (33).

$$2A_i^{d+2} + (d+2)\sigma^2 A_i^d - (d+2)A_c^d A_i^2 + dA_c^{d+2} - (d+2)\sigma^2 A_c^d = 0. \tag{33}$$

After $A_c$ and $A_i$ are obtained, both the companding function and the de-companding function are determined. With these functions, it is easy to perform companding and de-companding at the transmitter and the receiver, respectively.

By adjusting parameters $A_c$, $A_i$, and $d$, the PEC scheme can achieve various PAPR reduction levels. The profiles of PEC function with various parameters are shown in Fig. 8.

From (31), it is easy to see when $A_i = 0$ the PEC function degenerates into the EC function as follows,

$$h(x) = \operatorname{sgn}(x)\left[A_c^d\left(1 - e^{-|x_n|^2/\sigma^2}\right)\right]^{(1/d)}. \tag{34}$$

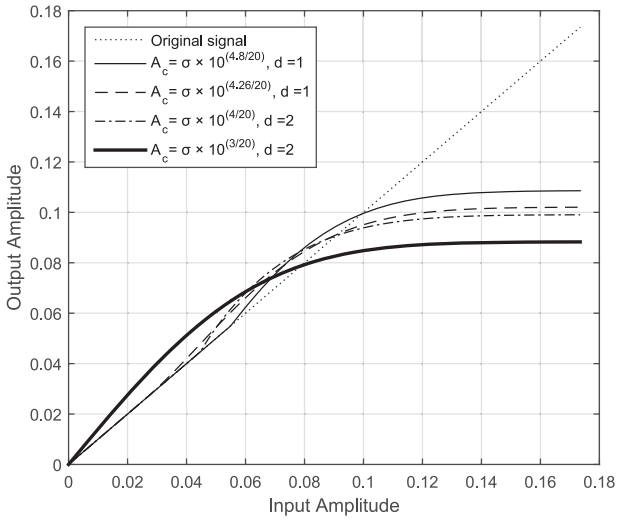


Fig. 8. Profiles of PEC function with different parameters.

We can adjust $A_c$ and $d$ to let the inflexion point $A_i$ be equal to 0. That is, the EC scheme is just a special case of the PEC scheme. Therefore, Elmaroud *et al.*'s [18] scheme which combines WHT precoding with EC is in fact a special case of the proposed scheme.

## IV. Simulation Results

To evaluate the performance of the proposed scheme, simulation results are presented in this section. In simulations, QPSK modulation is adopted, the number of subcarrier $N = 256$ and the length of cyclic prefix is 32. AWGN channels, six-ray Rayleigh fading channels, and six-ray Rice fading channels are applied in simulations.

With the consideration of algorithm complexity and system performance, the parameter $d$ of PEC is set to be the smallest value guaranteeing the average signal power constant for each value of $A_c$. So the PEC scheme with $A_c = \sigma \times 10^{(3/20)}$ and $d = 2$ is adopted.

In simulations, we compare the proposed hybrid scheme (FWF-OFDM with PEC) with traditional OFDM. Besides that, to show the effect of FWFT and PEC on system performance respectively, we make a comparison among FWF-OFDM, OFDM with PEC (Hu *et al.*'s [23] scheme) and traditional OFDM. Also, Xiao *et al.*'s [17] scheme which combines WHT precoding (WHT-OFDM) with $\mu$-law companding is used for comparison.

### *A. PAPR Reduction Performance*

When FWF-transform is adopted in OFDM systems, the superposition of the subcarriers is reduced due to the sparsity and block diagonal structure of the FWF-transform. So the peak of the transmitted signals is reduced while transmitted

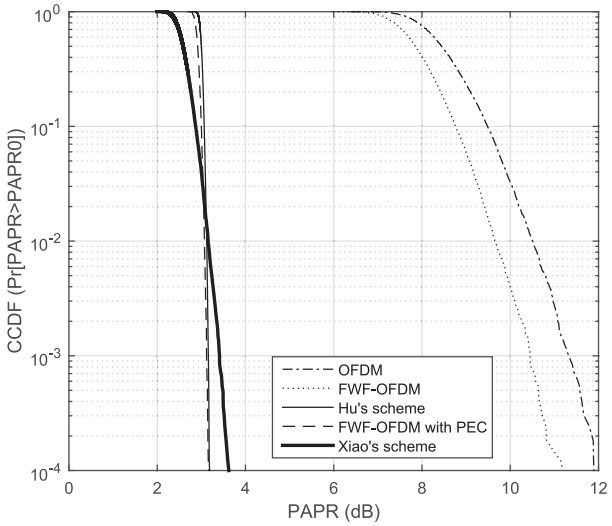


Fig. 9. CCDF performance of different OFDM systems with QPSK mapping.

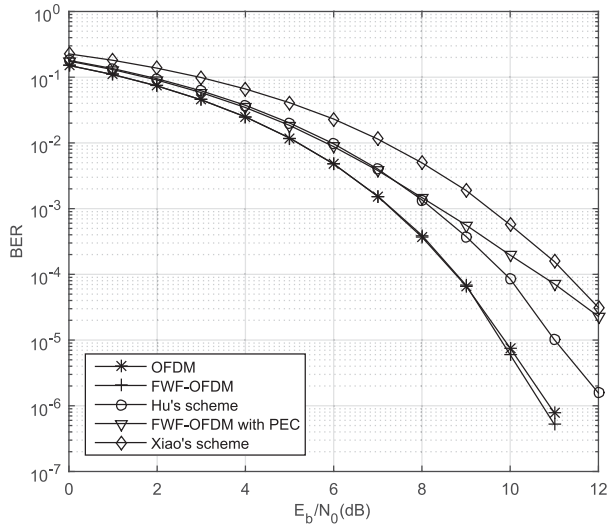


Fig. 10. BER performance of different OFDM systems in AWGN channels with QPSK mapping.

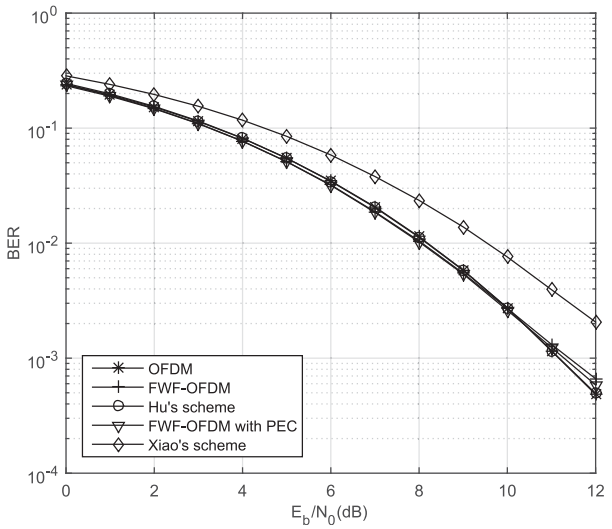


Fig. 11. BER performance of different OFDM systems with TWTA in AWGN channels with QPSK mapping.

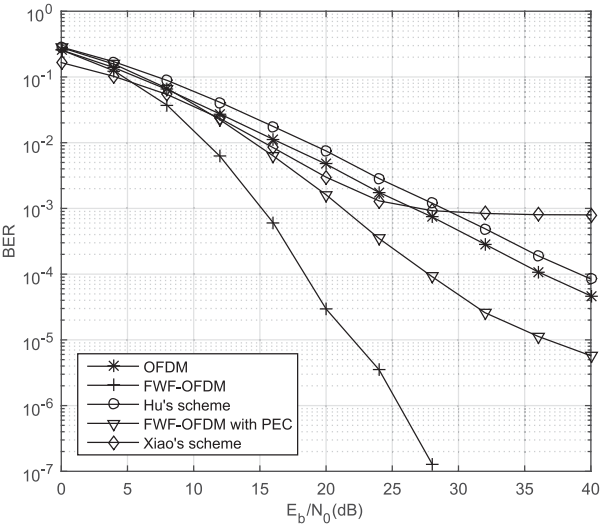


Fig. 12. BER performance of different OFDM systems in multipath Rayleigh fading channels with QPSK mapping.

average power maintains constant. As a result, the PAPR of OFDM signal is reduced. As Fig. 9 shows, the PAPR of the transmitted signal in FWF-OFDM is less than that of the traditional OFDM system by a range of 0.7∼0.9dB. In Fig. 9, we can also see that PEC can reduce PAPR significantly. When FWF-transform and PEC are combined, the hybrid method outperforms the two techniques individually.

Please note that to make a fair comparison of BER performance between the proposed hybrid scheme and Xiao's scheme, we adjust the parameter of $\mu$-law companding in Xiao's scheme for Xiao's scheme and the proposed hybrid method to achieve similar level of CCDF performance.

### *B. BER Performance*

The BER performance comparisons presented are accomplished with the assumptions of perfect frequency and time synchronization and known channel impulse responses. To evaluate the BER performance of these companded schemes, a travelling wave tube amplifier (TWTA), modeled as a memoryless non-linear amplifier, is adopted at the transmitter. Denote the input signal to TWTA as

$$x(t) = \rho(t) \cdot \exp\big[j\varphi(t)\big]. \tag{35}$$

The output signal of TWTA can be expressed as

$$y(t) = A[\rho(t)] \cdot \exp\big[j(\varphi(t) + \Phi[\rho(t)])\big], \tag{36}$$

where $A(\cdot)$ and $\Phi(\cdot)$ represent AM/AM and AM/PM distortions of the nonlinear amplifier, respectively. The AM/AM and AM/PM profiles of TWTA can be described as follows,

$$A[\rho(t)] = \frac{A_{sat}^2 \rho(t)}{\rho^2(t) + A_{sat}^2}, \tag{37}$$

$$\Phi[\rho(t)] = \frac{\pi}{3} \frac{\rho^2(t)}{\rho^2(t) + A_{sat}^2}, \tag{38}$$

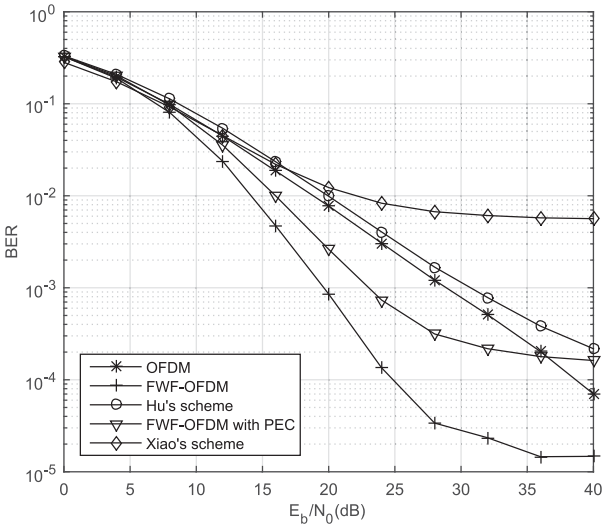


Fig. 13. BER performance of different OFDM systems with TWTA in multipath Rayleigh fading channels with QPSK mapping.

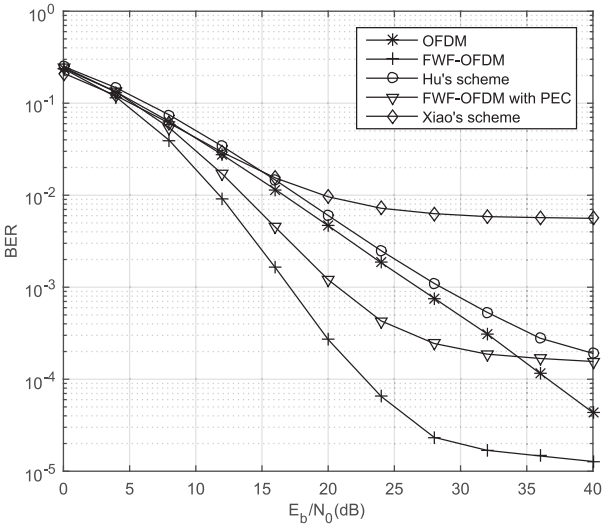


Fig. 15. BER performance of different OFDM systems with TWTA in multipath Rice fading channels with QPSK mapping.

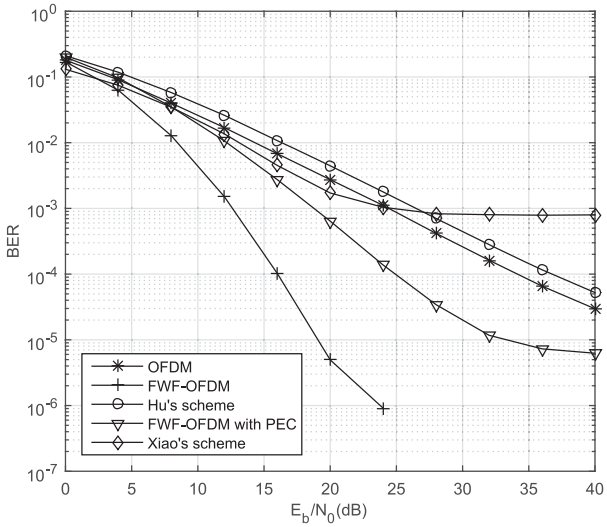


Fig. 14. BER performance of different OFDM systems in multipath Rice fading channels with QPSK mapping.

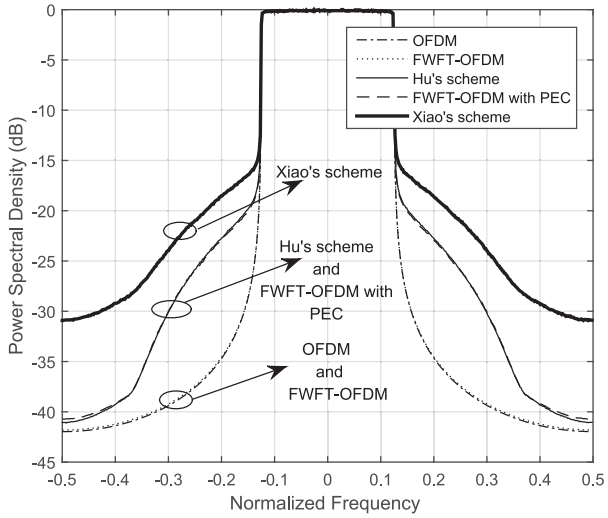


Fig. 16. PSD performance of different OFDM systems.

where $A_{sat}$ is the saturation level determined by the input back off (IBO) and the input signal power $\sigma^2$ (IBO $= 10\log(A_{sat}^2/\sigma^2)$). IBO is set to be 10 dB in simulations.

In FWF-OFDM, we employ FWF-transform which can use fast algorithm to calculate both Walsh-Hadamard and Fourier transforms efficiently. Adding Walsh-Hadamard to an OFDM system can increase frequency diversity and reduce the influence of the selective fading channel on system performance. As shown in Fig. 10 and Fig. 11, the BER performances of conventional OFDM and FWF-OFDM are nearly identical in AWGN channels. But when used in multipath fading channels, FWF-OFDM achieves significant BER performance improvement due to its high diversity gain which is clearly depicted in Figs. 12, 13 (multipath Rayleigh fading channels), and Figs. 14, 15 (multipath Rice fading channels with Rice factor k=5).

PEC is a non-linear processing, and may cause significant in-band distortion which causes bit error rate degradation. However, when PEC is adopted together with FWF-OFDM, in multipath fading channels, the hybrid system will not deteriorate but even improve the BER performance compared to conventional OFDM. Compared with Xiao's scheme, at the same PAPR reduction level, the BER performance of the proposed scheme is much better in both AWGN and multipath fading channels.

### C. PSD Performance

The power spectrum comparisons among the signals of different systems are shown in Fig. 16. We can see that FWF-OFDM achieves almost the same performance as conventional OFDM, which shows FWF-transform itself almost has no detrimental effect on the PSD performance. The PSD performance of OFDM and FWF-OFDM with PEC is worse

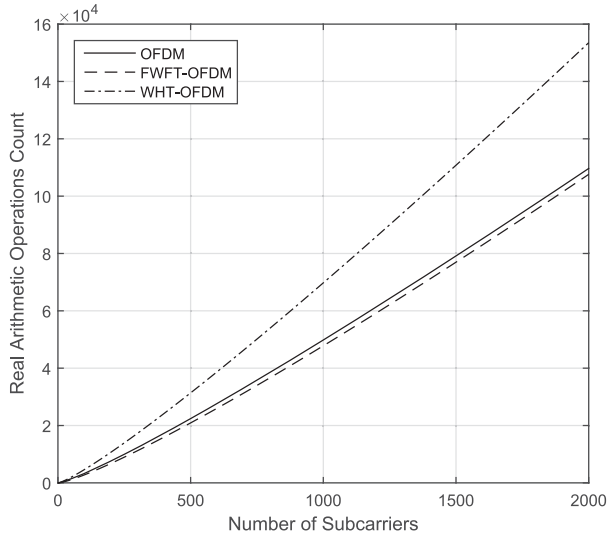


Fig. 17. Real arithmetic operations of different transforms.

than that of conventional OFDM because PEC is a lossy companding method which causes out of band spectrum regrowth. Compared with Xiao's scheme, the proposed scheme has a better PSD performance.

### D. Algorithm Complexity

Fig. 17 shows the FWF-transform involves less real arithmetic operations than transforms do in WHT-OFDM and conventional OFDM. As for companding techniques, a complexity comparison has been made between PEC and other companding techniques in [23] and showed that the overall complexity of the PEC scheme is lower than that of EC and Wang *et al.*'s [16] scheme. On the whole, the hybrid scheme has an advantage of low computational complexity.

## V. Conclusion

In this paper, we have proposed a hybrid system which combines FWFT with PEC. FWFT can achieve reasonable reduction in PAPR and significant improvement in BER with low complexity. Moreover, FWFT almost has no detrimental effects on the PSD performance. As for PEC, it can greatly improve the PAPR performance of the whole system while offering more design flexibility in the PAPR reduction. The hybrid method we have proposed combines the advantages and offsets the deficiency of the two techniques. From simulation results, we can see the proposed low complexity hybrid method outperforms existing methods when used in multipath fading channels.

## References

[1] X. Zhu, W. Pan, H. Li, and Y. Tang, "Simplified approach to optimized iterative clipping and filtering for PAPR reduction of OFDM signals," *IEEE Trans. Commun.*, vol. 61, no. 5, pp. 1891–1901, May 2013.

[2] Y.-C. Wang and Z.-Q. Luo, "Optimized iterative clipping and filtering for PAPR reduction of OFDM signals," *IEEE Trans. Commun.*, vol. 59, no. 1, pp. 33–37, Jan. 2011.

[3] S.-K. Deng and M.-C. Lin, "Recursive clipping and filtering with bounded distortion for PAPR reduction," *IEEE Trans. Commun.*, vol. 55, no. 1, pp. 227–230, Jan. 2007.

[4] X. Huang, J. H. Lu, J. L. Zheng, K. B. Letaief, and J. Gu, "Companding transform for reduction in peak-to-average power ratio of OFDM signals," *IEEE Trans. Wireless Commun.*, vol. 3, no. 6, pp. 2030–2039, Nov. 2004.

[5] Y. Wang, L.-H. Wang, J.-H. Ge, and B. Ai, "Nonlinear companding transform technique for reducing PAPR of ODFM signals," *IEEE Trans. Consum. Electron.*, vol. 58, no. 3, pp. 752–757, Aug. 2012.

[6] A. Ghassemi and T. A. Gulliver, "Intercarrier interference reduction in OFDM systems using low complexity selective mapping," *IEEE Trans. Commun.*, vol. 57, no. 6, pp. 1608–1611, Jun. 2009.

[7] H. Chen and H. Liang, "Combined selective mapping and binary cyclic codes for PAPR reduction in OFDM systems," *IEEE Trans. Wireless Commun.*, vol. 6, no. 10, pp. 3524–3528, Oct. 2007.

[8] K.-C. Chung, H. Chen, and T.-Y. Yang, "Low complexity PTS algorithms with error correction capability in OFDM systems," in *Proc. 7th Int. Conf. Ubiquitous Future Netw.*, Sapporo, Japan, 2015, pp. 254–256.

[9] T. Jiang, C. Ni, L. Guan, and Q. Qi, "Peak-to-average power ratio reduction in alamouti multi-input-multi-output orthogonal frequency division multiplexing systems without side information using phase offset based-partial transmit sequence scheme," *IET Commun.*, vol. 8, no. 5, pp. 564–570, Mar. 2014.

[10] M.-J. Hao and C.-H. Lai, "Precoding for PAPR reduction of OFDM signals with minimum error probability," *IEEE Trans. Broadcast.*, vol. 56, no. 1, pp. 120–128, Mar. 2010.

[11] J. Gao, X. Zhu, and A. K. Nandi, "Non-redundant precoding and PAPR reduction in MIMO OFDM systems with ICA based blind equalization," *IEEE Trans. Wireless Commun.*, vol. 8, no. 6, pp. 3038–3049, Jun. 2009.

[12] T. Jiang, Y. Yang, and Y.-H. Song, "Exponential companding technique for PAPR reduction in OFDM systems," *IEEE Trans. Broadcast.*, vol. 51, no. 2, pp. 244–248, Jun. 2005.

[13] T. Jiang, W. Xiang, P. C. Richardson, D. Qu, and G. Zhu, "On the nonlinear companding transform for reduction in PAPR of MCM signals," *IEEE Trans. Wireless Commun.*, vol. 6, no. 6, pp. 2017–2021, Jun. 2007.

[14] S.-S. Jeng and J.-M. Chen, "Efficient PAPR reduction in OFDM systems based on a companding technique with Trapezium distribution," *IEEE Trans. Broadcast.*, vol. 57, no. 2, pp. 291–298, Jun. 2011.

[15] J. Hou, J. Ge, D. Zhai, and J. Li, "Peak-to-average power ratio reduction of OFDM signals with nonlinear companding scheme," *IEEE Trans. Broadcast.*, vol. 56, no. 2, pp. 258–262, Jun. 2010.

[16] Y. Wang, L.-H. Wang, J.-H. Ge, and B. Ai, "An efficient nonlinear companding transform for reducing PAPR of OFDM signals," *IEEE Trans. Broadcast.*, vol. 58, no. 4, pp. 677–684, Dec. 2012.

[17] J. Xiao *et al.*, "Hadamard transform combined with companding transform technique for PAPR reduction in an optical direct-detection OFDM system," *IEEE/OSA J. Opt. Commun. Netw.*, vol. 4, no. 10, pp. 709–714, Oct. 2012.

[18] B. Elmaroud, A. Faqihi, M. Abbad, and D. Aboutajdine, "PAPR reduction of FBMC signals by combining exponential companding and Hadamard transforms," in *Proc. Int. Symp. Netw. Comput. Commun.*, Hammamet, Tunisia, 2014, pp. 1–4.

[19] Z. Wang, S. Zhang, and B. Qiu, "PAPR reduction of OFDM signal by using Hadamard transform in companding techniques," in *Proc. 12th IEEE Int. Conf. Commun. Technol. (ICCT)*, Nanjing, China, 2010, pp. 320–323.

[20] D. Agarwal, N. Sharan, M. P. Raja, and A. Agarwal, "PAPR reduction using precoding and companding techniques for OFDM systems," in *Proc. Int. Conf. Adv. Comput. Eng. Appl. (ICACEA)*, Ghaziabad, India, 2015, pp. 18–23.

[21] Z. Dlugaszewski and K. Wesolowski, "WHT/OFDM—An improved OFDM transmission method for selective fading channels," in *Proc. Symp. Commun. Veh. Technol. (SCVT)*, Leuven, Belgium, 2000, pp. 144–149.

[22] B. Gaffney and A. D. Fagan, "Walsh Hadamard transform precoded MB-OFDM: An improved high data rate ultrawideband system," in *Proc. IEEE 17th Int. Symp. Pers. Indoor Mobile Radio Commun.*, Helsinki, Finland, 2006, pp. 1–5.

[23] M. Hu, Y. Li, Y. Liu, and H. Zhang, "Parameter-adjustable piecewise exponential companding scheme for peak-to-average power ratio reduction in orthogonal frequency division multiplexing systems," *IET Commun.*, vol. 8, no. 4, pp. 530–536, Mar. 2014.

[24] S. Boussakta and A. G. J. Holt, "Fast algorithm for calculation of both Walsh-Hadamard and Fourier transforms (FWFTs)," *Electron. Lett.*, vol. 25, no. 20, pp. 1352–1354, Sep. 1989.

**Ce Kang** received the B.S. degree in communication engineering from Xidian University, Xi'an, China, in 2014. His current research interests lie in communications and signal processing, OFDM wireless communications, and full-duplex communications.

**Yi Liu** received the B.S. degree in communication engineering from Dalian Jiaotong University, Dalian, China, in 2002, and the M.S. and Ph.D. degrees in communication engineering from Xidian University, Xi'an, China, in 2005 and 2007, respectively. Since 2008, he has been with Xidian University, Xi'an, China. From 2011 to 2012, he was a Visiting Scholar with the University of Delaware, USA. He is currently a Professor with Xidian University. His research interests are in signal processing for wireless communications, MIMO and OFDM wireless communications, and full-duplex cooperative communications.

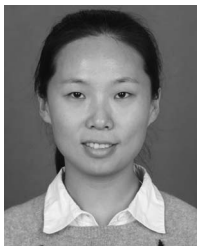

**Meixia Hu** received the Ph.D. degree in communications and information systems from Xidian University, Xi'an, China, in 2014. Her research interests include signal processing for wireless communications, MIMO and OFDM wireless communications, and cooperative communications.

**Hailin Zhang** received the B.S. and M.S. degrees from Northwestern Polytechnic University, Xi'an, China, in 1985 and 1988, respectively, and the Ph.D. degree from Xidian University, Xi'an, China, in 1991. Since 1991, he has been with Xidian University, where he is currently a Senior Professor and the Ph.D. Adviser with the School of Telecommunications Engineering. He is currently the Director of the Key Laboratory in Wireless Communications Sponsored by China Ministry of Information Technology, a Key Member of the State Key Laboratory of Integrated Services Networks, one of the state government specially compensated Scientists and Engineers, a Field Leader with Telecommunications and Information Systems, Xidian University, and an Associate Director for National 111 Project. He has recently published over 100 papers in telecommunications journals and proceedings. His current research interest includes key transmission technologies and standards on broadband wireless communications for 4G, 5G, and next generation broadband wireless access systems.